Neural basis for anxiety and anxiety-related physiological responses during simulated driving: An fMRI study

Takafumi Sasaoka[1], Tokiko Harada[1], Daichi Sato[2], Nanae Michida[2], Hironobu Yonezawa[2], Masatoshi Takayama[2], Takahide Nouzawa[3], Shigeto Yamawaki[1]

1. Center for Brain, Mind, and KANSEI Sciences Research, Hiroshima University, Japan.

2. Mazda Motor Corporation, Hiroshima Japan.

3.Office of Academic Research and Industry-Academia-Government and Community Collaboration, Hiroshima University, Japan.

Corresponding Author: Takafumi Sasaoka, PhD

Center for Brain, Mind, and KANSEI Sciences Research, Hiroshima University, 1-2-3 Kasumi, Minami-ku, Hiroshima, 734-8551, Japan.

Phone: +81-82-257-1722; Fax: +81-82-257-1723

E-mail: tsasaoka@hiroshima-u.ac.jp

Running Title: An fMRI study on the neural basis of anxiety

Abstract

While the exteroceptive and interoceptive prediction of a negative event increases a person's anxiety in daily life situations, the relationship between the brain mechanism of anxiety and anxiety-related autonomic response have not been fully understood. In this fMRI study, we examined the neural basis of anxiety and anxiety-related autonomic responses in a daily driving situation. Participants viewed a driving video clip in the first-person perspective. In the middle of the video clip, participants were presented with a cue to indicate whether a subsequent crash could occur (attention condition) or not (safe condition). Compared with the safe condition, there were more activities in the anterior insula, bed nucleus of the stria terminalis, thalamus, and periaqueductal gray, and higher sympathetic nerve responses, such as pupil dilation and peripheral arterial stiffness in the attention condition. We also observed autonomic response-related functional connectivity in the visual cortex, cerebellum, brainstem, and MCC/PCC with the right anterior insula and its adjacent regions as seed regions. Thus, the right anterior insula and adjacent regions, collaborating with the other related regions, could play a fundamental role in eliciting anxiety based on the prediction of negative events by mediating anxiety-related autonomic responses according to interoceptive information.

Keywords: anxiety, insula, peripheral arterial stiffness, pupillometry, sympathetic nerve response

Introduction

In recent years, it has been emphasized that the fundamental function of the brain, as a "prediction machine," is prediction and prediction error processing (e.g., Clark 2013). The predictive coding theory (Friston 2005; Rao and Ballard 1999) has been proposed as a computational framework for the brain prediction and prediction error processing, in which the brain works on the computational principle to minimize the difference between the prediction of the cause of the sensory input and the actual sensory input (prediction error). To minimize prediction errors, predictions are updated, or actions are performed to change the sensory input and to confirm the predictions (active inference); therefore, the cause of the sensory input is inferred. Based on this theory, perception could be regarded as an inference of the cause of external sensation (i.e., exteroception) in the outer world by prediction and prediction-error processing of exteroception (Rao and Ballard 1999). Likewise, subjective feelings could be regarded as an inference of the cause of the bodily sensation (i.e., interoception) by prediction and prediction-error processing of interoception (e.g., Seth, 2013, Barrett and Simmons, 2015; Barrett et al., 2016; Barrett, 2017).

Anxiety is a typical example of brain prediction processing. Anxiety can be defined by anticipatory affective, cognitive, and behavioral changes in response to uncertainty regarding potential threats (Grupe and Nitshke 2013). When the brain predicts a threatening event, which

can disturb homeostasis, negative emotions are elicited and attention is directed to the incoming information; thus, actions are undertaken to avoid the event. This corresponds to a state of anxiety.

Previous neuroscientific research on anxiety has suggested that the salience network (SN), including the insula, amygdala, and thalamus, and the extended amygdala, such as the bed nucleus of the stria terminalis (BNST), plays a crucial role in anxiety (e.g., Somerville et al. 2013). Hyperactivation in the insula is suggested to be related to anxiety disorders (Paulus and Stein 2006, 2010). Paulus and Stein (2006) proposed a hypothesis that individuals who are prone to anxiety show an altered interoceptive prediction generated in the anterior insula. Excessive interoceptive prediction could result in additional resources for the brain to reduce the prediction error between the observed and expected body states. Interoceptive information is often first processed in the brainstem, such as the medial nucleus of the solitary tract, the parabrachial nucleus, and relayed to the insula by the thalamus (Chen et al. 2021). The anterior insula has been suggested to be involved in the integration of interoceptive and exteroceptive representations, and updating them based on the incoming information (Craig 2009). Based on these observations, we can speculate that perception of a cue associated with threatening events triggers a prediction of negative body state generated by the anterior insula, and that accompanying interoceptive information is processed by the subcortical regions, such as the thalamus and brainstem.

The interoception processing model based on the predictive coding theory (Seth 2013) assumes that the prediction of upcoming threatening events results in updating the desired state of the organism, accompanied by autonomic reflexes. It is well known that autonomic responses, such as increasing heartbeats (e.g., Deane 1961), skin conductance (e.g., Epstein and Roupenian 1970), and pupil dilation (e.g., Bitsios et al. 2004) are observed when people experience anxiety. However, only few studies examining the brain mechanisms involved in the autonomic responses related to anxiety exist. For instance, Wager et al. (2009a, 2009b) reported that the dorsal pregenual cingulate region was active in relation to the increase in the heart rate while facing a socially threatening situation in which participants were going to deliver a speech to others. However, many other indices exist that reflect sympathetic nerve activity rather than the heart rate. Peripheral arterial stiffness (β_{art}) has been proposed (Matsubara et al. 2018; Tsuji et al. 2021) as an index reflecting sympathetic activity. β_{art} can be estimated using electrocardiography, continuous sphygmomanometry, and photoplethysmography. Tsuji et al. (2021) demonstrated that β_{art} correlated with subjective pain ratings and brain activity in regions, including the SN (e.g., dorsal anterior cingulate cortex), thereby suggesting that β_{art} is a potential candidate for a sympathetic nerve index reflecting anxiety based on neuroscientific evidence.

Clarifying the neural basis for eliciting anxiety and for accompanying autonomic responses in a daily situation will lead to understanding the mechanism of anxiety and anxiety

disorders, as well as implementing a system to appropriately reduce anxiety by reading out anxiety-related autonomic responses. Therefore, based on the definition by Somerville et al. (2013), in this paper, we defined "anxiety" as a lengthy emotional state induced by an anticipation of a potential threat in contrast with "transient fear." In the current study, we examined the brain mechanisms involved in eliciting anxiety by using stimuli simulated in a daily situation of driving a vehicle. Furthermore, to elucidate the neural substrates involved in autonomic responses related to anxiety, we performed simultaneous measurements of functional magnetic resonance imaging (fMRI) and physiological indices, such as electrocardiogram (ECG), photoplethysmogram (PPG), blood pressure, and pupillometry. In particular, we focused on pupil dilation and β_{art} as indices that putatively reflect sympathetic nerve activity. In the experiment, participants performed a simple reaction task while watching a simulated driving video clip in the MRI scanner. In the middle of the video clip, participants were visually presented with a cue to indicate whether a car crash may subsequently occur (the word "Attention") or not (the word "Safe"). There were three conditions: a cue "Attention" was followed by a car crash (crash condition) or followed by no car crash (attention condition), and a cue "Safe" was followed by no car crash (safe condition). We hypothesized that the anterior insula and subcortical regions involved in threat and interoceptive processing, such as the BNST, amygdala, thalamus, and midbrain, are active following the cue "Attention" compared to following the cue "Safe." Moreover, we predicted significant

physiological responses indicating the sympathetic nerve activity (β_{art} and pupillary dilation) following the cue "Attention," which would modulate functional connectivity between the anterior insula and other brain regions.

Materials and Methods

Participants

Thirty-four healthy adult participants completed this experiment (4 females, all right-handed, aged 23.0 ± 2.12). All the participants had a driver's license and drove a car at least once a week. None of the participants had a history of mental disorders. All the participants provided written informed consent prior to participating in the study. This study was approved by the Research Ethics Committee of Hiroshima University (approval number E-965-3).

Experimental design

Figure 1 shows a schematic of the experimental trial. In the experiment, participants viewed a first-person perspective driving video clip generated by a driving simulator (D3sim, Mitsubishi Precision Co., Ltd., Japan). The video clip displayed a vehicle advancing through a narrow street for 26–28 s. At 17 s following the onset of the video clip,

either the word “Attention” or “Safe” was superimposed for 2 s on the video clip. Among the 16 trials in which the word “Attention” appeared, six revealed a scooter approaching and hitting the vehicle, with the presentation of a broken windshield and a collision sound (crash condition). In contrast, no scooter was seen approaching the vehicle in the remaining 10 trials (attention condition) and in the 16 trials in which the word “Safe” appeared (safe condition). At the end of each trial, the word “STOP” was displayed for 1 s, the participants were subsequently asked to press a button with their right index finger similar to a hard-braking event. The timing of the presentation of “STOP” was randomized within 26–28 s following the video clip onset. Participants were presented with the word “GOOD” or “BAD” as a feedback to indicate whether they could respond in 1 s from the presentation of “STOP.” We defined the 10-s period from the video clip onset as the “baseline” period and the 8-s period from the cue onset as the “anticipation” period.

After each trial, participants rated four items (anxiety, pleasantness, unpleasantness, and arousal) assessing their affective states during the anticipation period using a visual analog scale (VAS). For each item, the participants moved a cursor to indicate their rating (from 0 to 100) by pressing buttons with their middle and ring fingers. The experiment consisted of four sessions with eight trials each. Prior to the main trials, the participants performed three practice trials (one trial for each condition). Trait and state anxiety scores were obtained using the State-Trait

Anxiety Inventory. Trait anxiety scores were obtained prior to the experiment. State anxiety scores were obtained before and after the experiment.

Visual stimuli were presented on an MRI-compatible 32-inch liquid crystal display (NordicNeuroLab, Bergen, Norway) with a resolution of 1,920 × 1,080 pixels that subtended 30.4°× 17.4° visual angles. The participants viewed the visual stimuli through a mirror attached to the head coil. Auditory stimuli were presented with MRI-compatible noise-canceling headphones (OptoActive, Optoacoustics Ltd, Or Yehuda, Israel). The volume of the auditory stimuli was adjusted to ensure that it was not too loud based on the participants' self-reports during the practice trials.

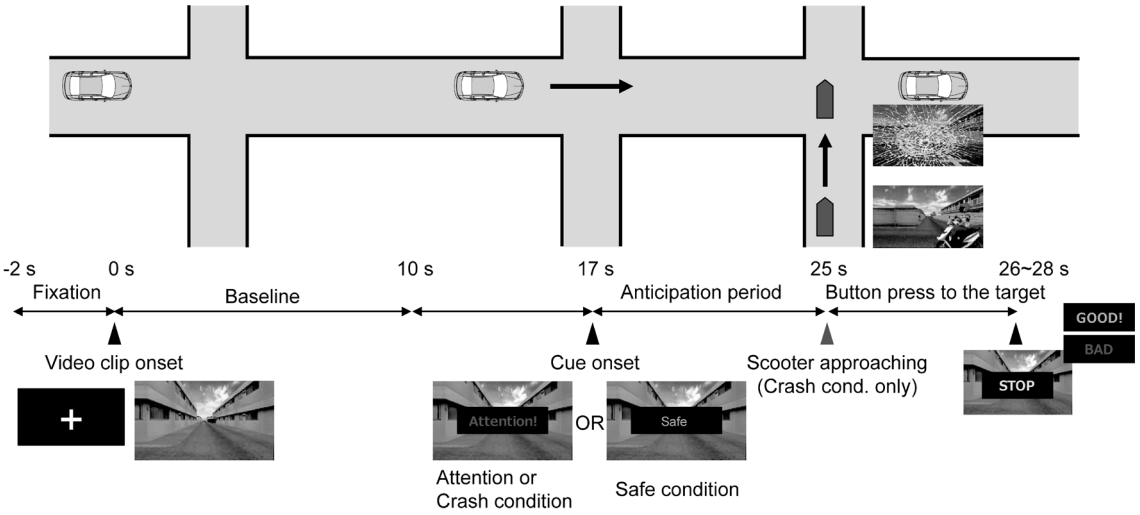

Figure 1. Schematic timeline of an experimental trial. In each trial, participants were presented with a first-person perspective driving video clip. At 17 s following the video clip onset, participants were presented with a word "Attention" or "Safe" for 2 s as a cue to indicate whether

a subsequent crash is possible to occur (attention /crash condition) or not (safe condition). In the crash condition, a scooter approached and hit the vehicle at 25 s following the video-clip onset. At the end of a video-clip, "STOP" was presented for 1 s, and participants were asked to press a button as quickly as possible. As a feedback whether their response was performed within 1 s following the presentation of "STOP," "GOOD," or "BAD" was presented. We defined 10-s period from the video clip onset as "baseline," and 8-s period from the cue onset as "anticipation period." See "Materials and Method" for details.

Analysis of behavioral data

The subjective rating data for each item were z-score normalized for each participant. To examine the differences in ratings among conditions and the occurrence of habituation, we performed a two-way repeated measures analysis of variance (ANOVA) with factors of task condition and session for each item.

The reaction time (RT) data for each participant were averaged for each condition. To examine whether there were any differences in the mean RT, we performed a one-way repeated measures ANOVA with a factor of task condition. If any main effects or interactions were significant, we performed a post-hoc test using the modified Shaffer method.

Acquisition and analyses of autonomic responses

To examine autonomic responses related to the participants' anxiety, we measured the pupil area, ECG, PPG, and blood pressure.

Pupil area

The pupil area of the participants' right eye was monitored using an MRI-compatible eye tracker (EyeLink 1000 Plus, SR Research, Osgoode, ON, Canada) at a sampling rate of 500 Hz. The pupil data were analyzed within the period from -2 s to 25 s around the onset of the video clip (0 s). Data for one participant and six out of the remaining 132 sessions (33 participants × 4 sessions) were excluded from the statistical analysis owing to excessive eyeblinks and measurement artifacts based on visual inspection. The data 200 ms before and following the eye blinks were replaced with Not-a-Number (NaN) since the data within this period were possibly contaminated by eye blinks (Choe et al. 2016). To examine when the difference was statistically significant in the trial, we performed a paired *t*-test on the mean pupil areas between the conditions at each time point throughout the trial. Since we expected that the difference in the autonomic responses between the attention and safe conditions will be observed during the

anticipation period, and that the presentation of a cue itself could affect the autonomic responses just following the cue onset, we also calculated the mean pupil areas over the 5-s period from 3 s to 8 s following cue onset (20–25 s following video clip onset), and then compared them between conditions using a paired *t*-test. Since we focused on the period before the crash (25 s following video clip onset), the crash and attention conditions were collapsed (crash/attention condition) in this analysis.

Peripheral arterial stiffness

ECG signals were acquired from a three-lead electrocardiograph placed on the participant's chest. A photoplethysmograph was attached to the participant's left index finger. Systolic blood pressure and diastolic blood pressure values during a single heartbeat were measured using the Care Taker module of Biopac Systems (Biopac Systems, Goleta, CA). A blood pressure cuff was attached to the participant's left thumb. These physiological signals were recorded using a Biopac MP 150 system at a sampling rate of 1000 Hz. Since data could not be obtained from one participant owing to a problem in the measurement device, the data of 33 participants were used for the statistical analysis. β_{art} was calculated at each single heartbeat timing based on the following equation (Tsuji et al. 2021):

$$\beta_{art} = \frac{\ln\left(\frac{P_{SYS}}{P_{DIA}}\right)}{P_{lmax} - P_{lmin}} \quad (1)$$

where P_{lmax} and P_{lmin} are the maximum and minimum values of the PPG within a heartbeat, respectively. P_{SYS} and P_{DIA} are systolic and diastolic blood pressures within a heartbeat. Using this equation, β_{art} was calculated for each heartbeat. The measured ECG was used to determine the R–R interval for extracting the P_{SYS}, P_{DIA}, P_{lmax}, and P_{lmin} for each heartbeat. However, we could not robustly detect the R peaks in the measured ECG data obtained from most participants owing to MRI artifacts. Therefore, we used the inverted PPG waveforms for each participant and segmented the waveform between two adjacent peaks to determine each heartbeat.

To compare the β_{art} between the conditions, we calculated the ratio of the mean β_{art} averaged over the 5-s period from 3 s to 8 s following cue onset (20 s following video clip onset) to the mean β_{art} averaged over the baseline, and subsequently performed a paired *t*-test.

MRI data acquisition

MRI data were acquired using a 3.0T MRI scanner (Siemens Magnetom Verio). The functional images were acquired using echo-planar T2*-weighted multiband gradient echo sequence with the following parameters: repetition time (TR), 1000 ms; echo time (TE), 30.00 ms; voxel size, 3.0 ×3.0 ×3.2 mm; 42 slices; slice thickness, 3.2 mm; field of view (FOV), 192

mm; flip angle, 80º; and acceleration factor, 3. The structural image of each participant was acquired using T1-weighted, three-dimensional magnetization prepared rapid gradient echo imaging (MPRAGE) with the following parameters: TR = 2300 ms, TE = 2.98 ms, voxel size = 1.0 ×1.0 ×1.0 mm, flip angle = 9 °, and FOV = 256 mm.

MRI data analysis

MRI data preprocessing and statistical analyses were performed using SPM12 software (Wellcome Department of Cognitive Neurology, London, UK www.fil.ion.ucl.ac.uk/spm). The first 10 volumes were discarded to permit T1 equilibration effects. In order to account for the correction of the head movement, the remaining volumes were spatially realigned to the first of the volumes and realigned to the mean of all the images. T1-weighted structural images were co-registered with the first echo-planar images (EPIs). The co-registered structural images were spatially normalized to the Montreal Neurological Institute (MNI) template. The parameters derived from this normalization process were subsequently applied to each EPI. The normalized EPIs were spatially smoothed using an 8-mm full width at half maximum Gaussian kernel.

Voxel-based statistical analysis of the pre-processed EPIs was performed using a general linear model (GLM). The blood oxygenation level-dependent (BOLD) response was related to

the baseline and anticipation periods, and the crash events were modeled as a box-car function for the onset and duration of each event (10 s for the baseline, 8 s for the anticipation period, and 0 s for the crash event). Each resulting time series for each event was convolved with a canonical hemodynamic response function and then used as a regressor. Six head motion parameters derived from the realignment process were also used as regressors to reduce motion-related artifacts. To eliminate low-frequency drifts, a high-pass filter with a 128-s cut-off period was applied to the fMRI time series. Serial autocorrelations between scans were corrected using a first-order autoregressive model.

Regression coefficients for each event were computed for each participant using a fixed-effects model. We created contrast images for the anticipation periods relative to the baseline in each of the crash, attention, and safe conditions, and the contrast images to compare the brain activity during the anticipation period between the attention and safe conditions. We also created contrast images for the crash events relative to the baseline. These contrast images were then subjected to group analysis using a random-effects model with a one-sample *t*-test. In the group analysis, we set the statistical threshold at uncorrected $p < 0.001$ at the voxel level and family wise error (FWE) corrected $p < 0.05$ at the cluster level. From the following main analyses (for the common brain activity during the anticipation period, the difference in brain activity during the anticipation period between the conditions, and the parametric modulation analyses), we

excluded the crash condition (i.e., the condition in which a cue "Attention" was followed by a car crash) based on the following reasons: (1) the crash condition contained the presentation of a broken windshield and a collision sound, unlike the attention and safe conditions; (2) since subjective ratings were obtained after each trial, it is possible that the additional aversive auditory-visual information affected the subjective ratings in the crash condition.

To examine subjective anxiety-related brain activity, we conducted parametric modulation analyses. For parametric modulation of subjective anxiety, we used regressors for the anticipation period in the trials under both attention and safe conditions, and z-score normalized scores of anxiety for each corresponding trial.

Autonomic response-related functional connectivity analysis

To examine the pupil- and β_{art}- related brain network, we examined functional connectivity (FC) between the anterior insula and its adjacent regions (as seed regions) and rest of the brain regions by conducting a generalized form of context-dependent psychophysiological interactions (gPPI) using CONN toolbox (Whitfield-Gabrieli and Nieto-Castanon, 2012). For gPPI analyses, we created GLMs including a regressor for the anticipation period in trials under both attention and safe conditions. The processed GLM for each participant was imported to the

gPPI model in the CONN toolbox. For each participant, we created a separate gPPI model for each of pupil area and β_{art} parametric modulators. As first-level covariates, we created gPPI regressors using parametric-modulation time-series based on trial-by-trial values of the ratio of mean β_{art} and pupil area averaged over the 5-s period from 3 s to 8 s following the cue onset to those averaged over the baseline. Based on our hypothesis, we defined seed regions as the anterior insula (dorsal and ventral agranular insula) and the anatomical regions in the cluster, including the anterior insula activated in the contrast condition (attention > safe). We used Human Brainnetome Atlas (Fan et al, 2016) to define these anatomical ROIs. In the second-level analysis, seed-based connectivity maps of Fisher-transformed correlation coefficients between BOLD time-series of each seed region and each individual voxel were entered into a one-sample *t*-test to examine the brain region showing significant pupil- and β_{art}-related FC with each seed region. We applied the statistical threshold at uncorrected $p < 0.001$ at the voxel level and false discovery rate (FDR) corrected $p < 0.05$ at the cluster level.

Results

Behavioral data

Subjective ratings

Figure 2 shows the results of subjective ratings. Regarding subjective rating of anxiety, a repeated-measures two-way ANOVA with factors of task conditions (crash, attention, and safe) and session (sessions 1, 2, 3, and 4) revealed a significant main effect of task conditions (F [1.84, 60.83] = 316.596, partial η^2 = .906, $p_{corrected} < 0.001$, Chi-Muller correction for non-sphericity was applied). Post-hoc analyses using the modified Shaffer method revealed that the participants rated subjective anxiety highest in the crash condition, followed by the attention condition, and the safe condition (all ts [33] > 4.281, all ps < 0.001). In contrast, we observed no main effect of session (F [2.40, 79.08] = 0.423, partial η^2 = 0.013, $p_{corrected}$ = 0.693) or interaction (F [5.35, 176.41] = 0.786, partial η^2 = 0.023, $p_{corrected}$ = 0.569). Considering the unpleasantness and arousal, repeated-measures two-way ANOVA also revealed a significant main effect of condition (unpleasantness: F [2, 66] = 304.478, partial η^2 = 0.902, $p_{corrected}$ < 0.001; arousal: F [2, 66] = 156.673, partial η^2 = 0.826, $p_{corrected} < 0.001$); however, no main effect of session (unpleasantness: F [2.64, 86.96] = 1.004, partial η^2 = 0.03, $p_{corrected}$ = 0.388; arousal: F [2.54, 83.78] = 0.696, partial η^2 = 0.021, $p_{corrected}$ = 0.534) or interaction (unpleasantness: F [4.93, 162.75] = 0.898, partial η^2 = 0.026, $p_{corrected}$ = 0.483; arousal: F [4.99, 164.57] = 1.316, partial η^2 = 0.038, $p_{corrected}$ = 0.260) was observed. Post-hoc analyses again replicated the result for anxiety (unpleasantness: all ts [33] > 10.207, $p < 0.001$; arousal: all ts [33] > 3.002, all ps < 0.01). Considering pleasantness, a repeated-measures two-way ANOVA

again revealed a significant main effect of condition (F [1.94, 63.91] = 213.201, partial η^2 = 0.866, $p_{corrected} < 0.001$). Post-hoc analyses revealed that pleasantness was rated highest in the safe condition, followed by the attention condition, and the crash condition (all ts [33] > 9.249, all ps < 0.001). We observed no main effect of session (F [3, 99] = 1.005, partial η^2 = 0.03, $p_{corrected}$ = 0.394); however, a marginally significant interaction (F [4.89, 161.29] = 2.098, partial η^2 = 0.06, $p_{corrected}$ = 0.07) was observed.

The mean scores of STAI-trait, and STAI-state before (STAI-state pre) and after the experiment (STAI-state post) were as follows: STAI-trait, 42.5 ± 7.50; STAI-state pre, 35.29 ± 7.50; and STAI-state post, 34.82 ± 6.80. We conducted correlation analyses between all pairs of the mean subjective ratings for each participant for each item and the score of STAI (STAI-trait, STAI-state pre, and STAI-state post). No significant correlation was observed between all the pairs (all ps > 0.10).

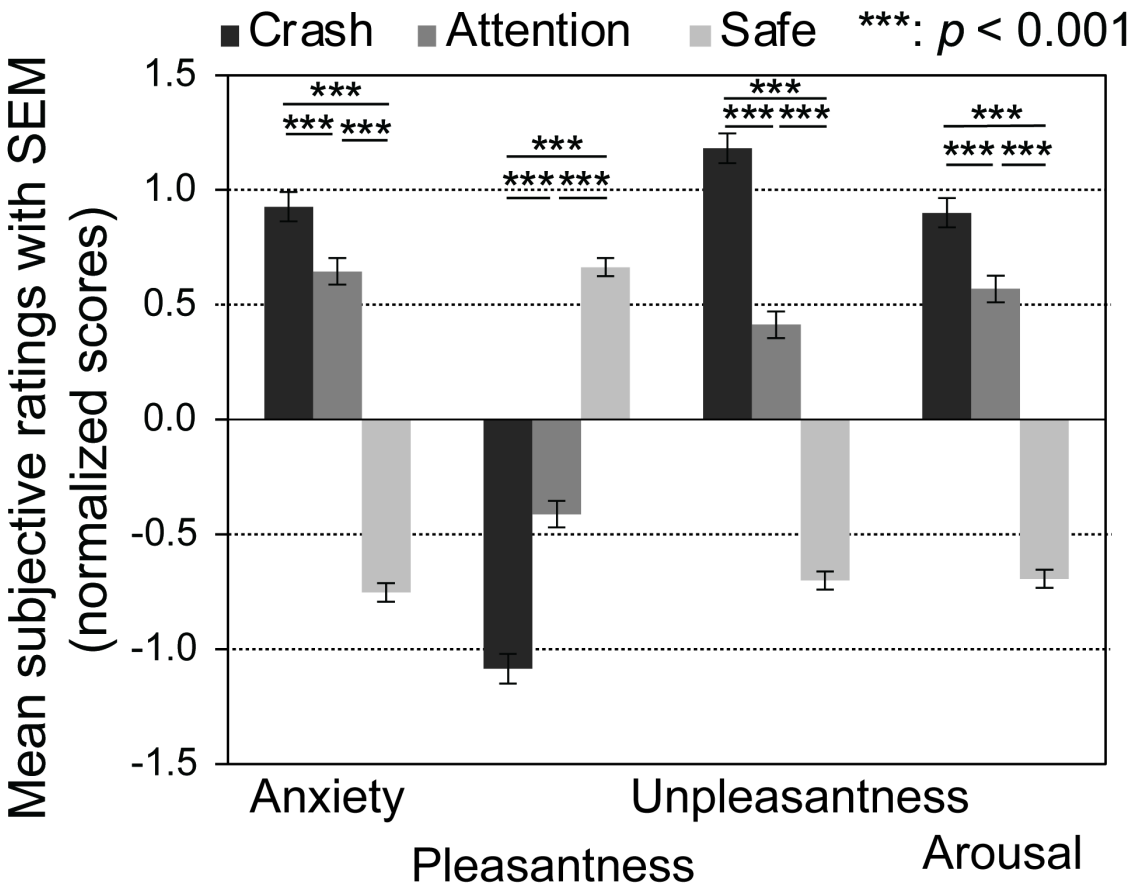

Fig. 2. The result of subjective ratings. SEM, standard error of the mean.

Reaction times

Figure 3 shows the mean RT for each condition. A one-way ANOVA on the mean RTs with a factor of task condition revealed a significant main effect (F [1.73, 57.07] = 17.793, partial η^2 = 0.350, $p_{corrected} < 0.001$). Post-hoc analyses using the modified Shaffer method revealed that the mean RT for the crash condition was faster than that for the attention and safe conditions (ts [33] < -4.060, ps < 0.001). However, we found no significant difference between the attention and safe

conditions (t [33] = -1.070, p = 0.292).

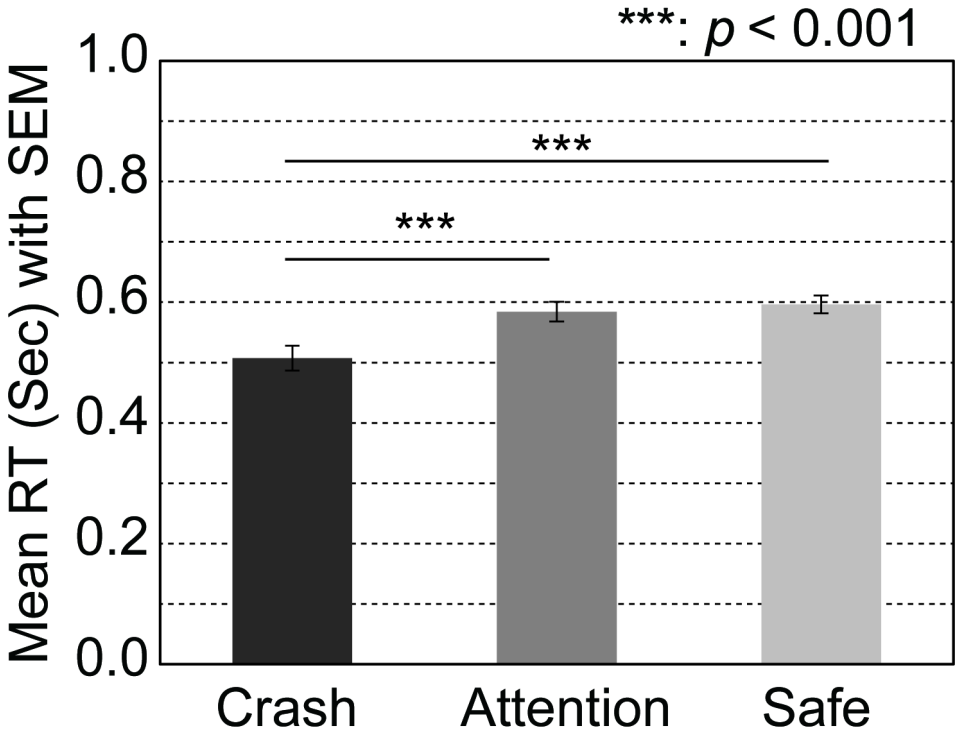

Fig. 3. Mean reaction time. SEM, standard error of the mean.

Autonomic responses

Pupil dilation

Figure 4 shows the mean time series of all the participants' pupil responses during the task for each condition. For data at each time point, we performed a paired t-test (corrected for multiple comparisons using an adjusted p-value threshold calculated to control the FDR). This revealed significantly more pupil dilation in the crash/attention conditions than in the safe

condition at the threshold of $p_{FDR} < 0.05$, mainly in the period from approximately 1 s following the cue onset (i.e., 18 s following the video clip onset) to the end of the trial. The gray areas in Figure 4 represent the time points showing significant differences between the conditions. This indicates that significant differences were robustly observed during the period from 3 s to 8 s following cue onset. To examine the statistical difference between conditions during this period, we performed a paired *t*-test between the mean pupil areas in the crash/attention and safe conditions in the period from 3 s to 8 s following the cue onset. This again revealed significantly more pupil dilation in the crash/attention condition than in the safe condition (t [33] = 4.4023, $p < 0.001$).

To examine the relationship between the pupil dilation and the subjective ratings of anxiety, we conducted a correlation analysis using the difference between the mean rating scores of anxiety in the attention and safe conditions for each participant and the difference between the mean pupil areas in the crash/attention and safe conditions in the period from 3 s to 8 s following the cue onset. A marginally significant positive correlation ($r = 0.313$, t [31] = 1.834, $p = 0.076$, Figure 5) was noted. In addition, we conducted a correlation analysis using the difference between the mean pupil areas excluding the crash condition. This again revealed a marginally significant positive correlation ($r = 0.294$, t [31] = 1.712, $p = 0.097$). For the other items, we found a marginal positive correlation for arousal ($r = 0.318$, t [31] = 1.865, p =

0.072); however, no significant correlation for pleasantness or unpleasantness (pleasantness: r = 0.270, t [31] = 1.564, p = 0.128; unpleasantness: r = 0.149, t [31] = 0.836, p = 0.409) was observed.

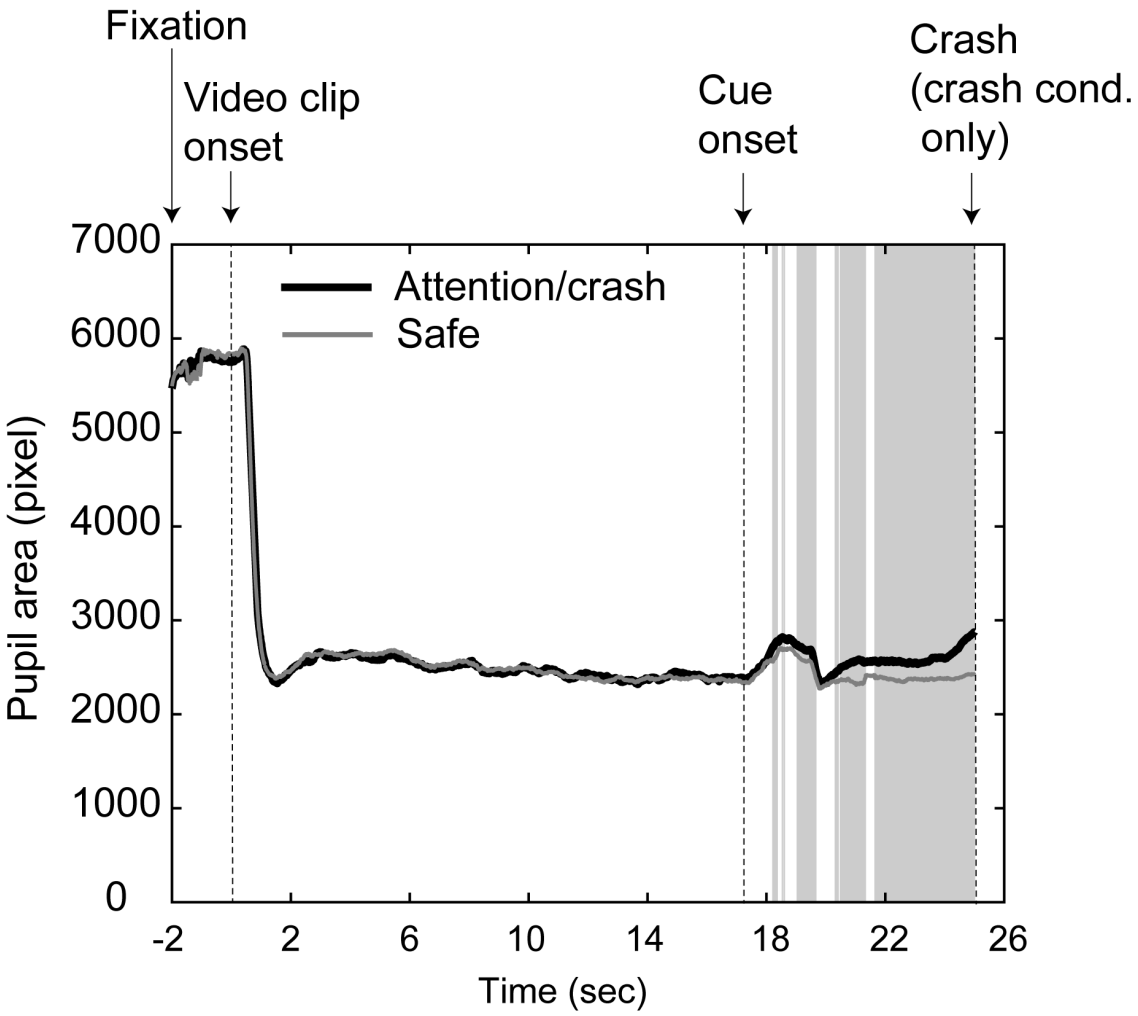

Fig. 4. The mean time-series of pupil areas for attention/crash and safe conditions. The gray areas represent the time point showing significant differences between conditions (see text).

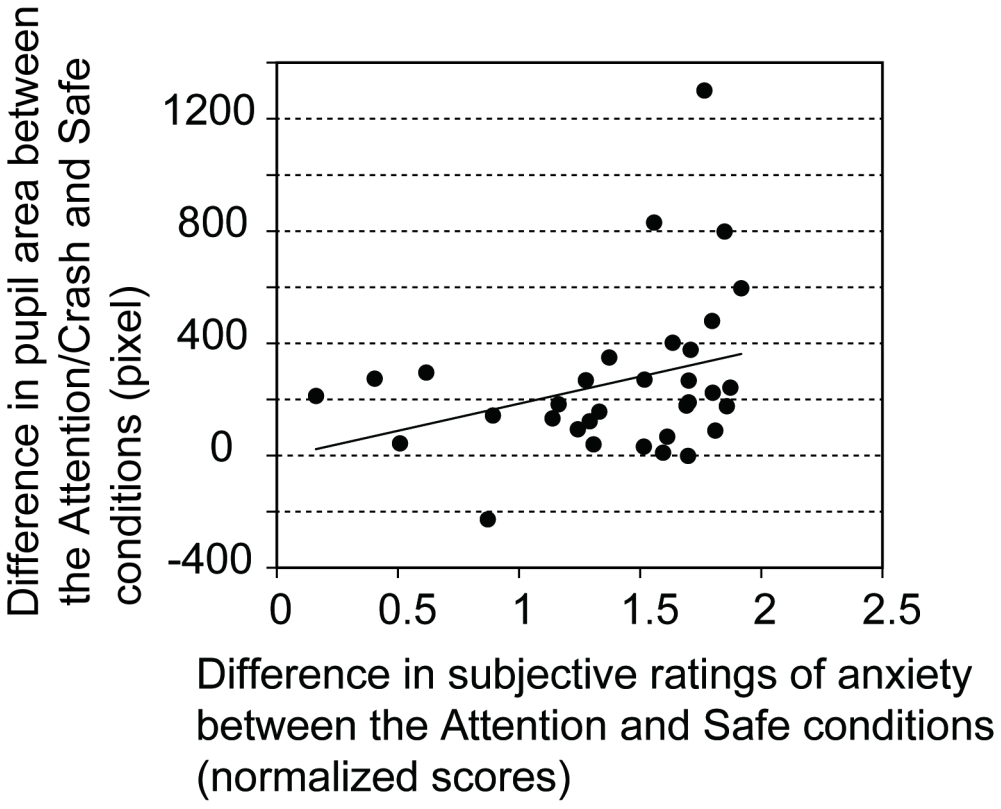

Fig. 5. Correlation between the difference in pupil areas between the attention/crash and safe conditions and the difference in subjective ratings of anxiety between the attention and safe conditions. The line represents the result of a linear regression.

Peripheral arterial stiffness

Figure 6 shows the mean time series of all the participants' β_{art} during the task for each condition. To examine the significance of the increase in β_{art} following cue onset, we compared the ratio of the mean value of β_{art} during the 5-s period from 3 s to 8 s following the cue onset to the mean value over the baseline between the attention and safe conditions using a paired *t*-test.

This revealed a tendency for β_{art} in the attention condition to be greater than in the safe condition (t (32) = 1.80, p = 0.08).

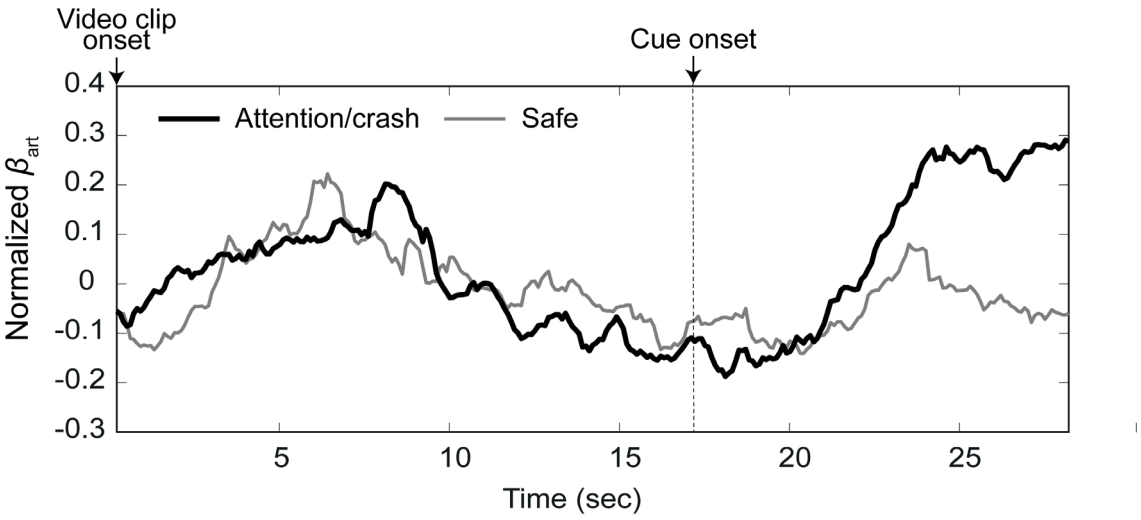

Fig. 6. The mean time-series of peripheral arterial stiffness (β_{art}) for attention/crash and safe conditions.

fMRI data

Brain activity during the anticipation period

To examine the common brain activity during the anticipation period relative to the baseline in both the attention and safe conditions, we conducted a conjunction analysis. This revealed significant activations in the bilateral front-parietal cortices, dorsal anterior cingulate cortex, and bilateral anterior insula (Figure 7, Table 1).

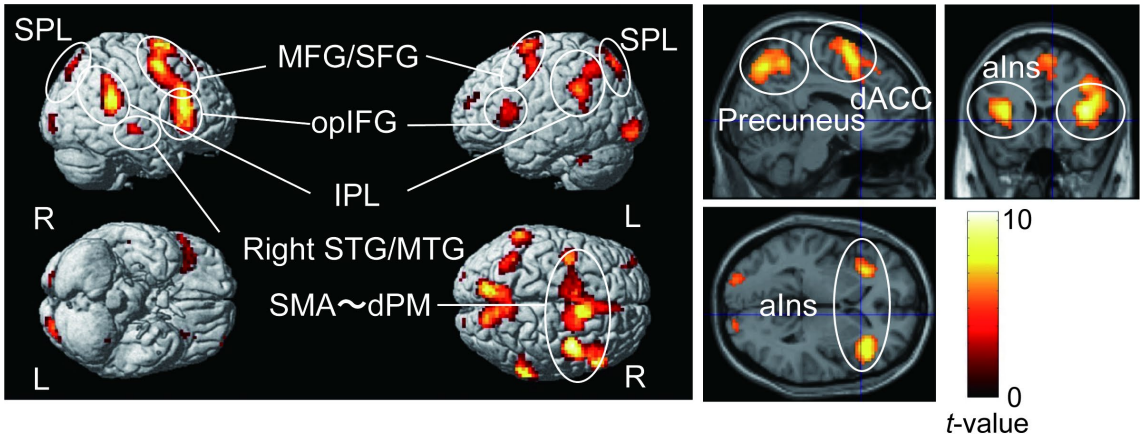

Fig. 7. Brain regions commonly activated in the attention and safe conditions revealed by a conjunction analysis. SPL, superior parietal lobule; Vis, visual cortex; MFG, middle frontal gyrus; SFG, superior frontal gyrus; opIFG, inferior frontal gyrus operculum part; SMA, supplementary motor area; dPM, dorsal premotor cortex; dACC, dorsal anterior cingulate cortex; aIns, anterior insula

Table 1. Common brain regions activated in both the attention and safe conditions during the anticipation period based on the result of a conjunction analysis.

Anatomical region	**Cluster size**	**MNI coordinates (mm)**			***T*-value**
		x	**y**	**Z**	
Left lingual gyrus	4299	-12	-88	-9	18.67

Right calcarine gyrus		12	-88	-3	17.87
Right lingual gyrus		21	-76	-12	15.84
Right superior frontal gyrus	1201	24	-1	61	9.34
Left superior frontal gyrus		-24	-4	68	8.41
Left supplementary motor area		-6	11	52	7.39
Right inferior frontal gyrus triangular part	116	60	23	16	5.35
Right inferior frontal gyrus triangular part / anterior insula		39	23	13	4.45
Left inferior frontal gyrus operculum part / left anterior insula	100	-45	14	10	5.15
Left inferior frontal gyrus operculum part / left anterior insula		-36	17	10	4.70

Uncorrected $p < 0.001$ at peak level, family wise error corrected $p < 0.05$ at the cluster level. MNI, Montreal Neurological Institute

To examine the brain regions related to each condition, we compared brain activation between the attention and safe conditions during the anticipation period. In the attention

condition, the right anterior insula and the sub-cortical regions, including the periaqueductal gray (PAG), thalamus, and the BNST were more active than in the safe condition (Figure 8, Table 2). In contrast, the areas from the parietal operculum, including the secondary somatosensory area (SII) to the posterior insula, and the precuneus were less active in the attention condition than in the safe condition. Although these areas were deactivated under all conditions, deactivation was more evident in the attention condition than in the safe condition (Figure 9, Table 3).

Parametric modulation using anxiety rating scores, including attention and safe conditions, revealed that activations in the thalamus and PAG positively correlated with the anxiety ratings. In contrast, we found no brain regions showing significant negative correlation with the anxiety ratings at the voxel-level threshold of uncorrected $p < 0.001$, cluster-corrected FWE $p < 0.05$, but at a liberal threshold, the SII and posterior insula showed a marginally significant negative correlation (voxel-level uncorrected $p < 0.005$; cluster-corrected FWE $p = 0.066$; Figure 10, Table 4).

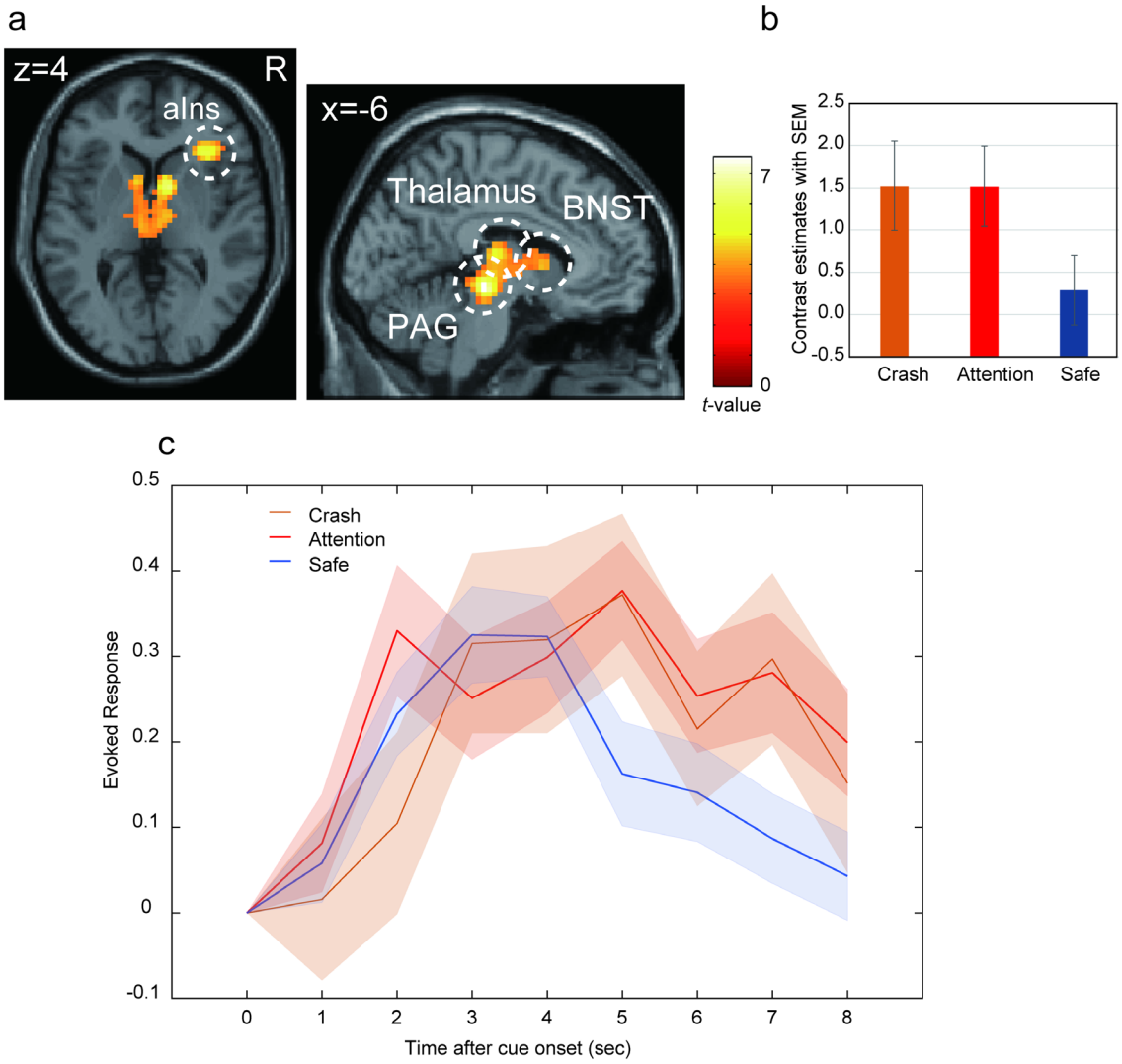

Fig. 8. (A) Brain regions more activated in the attention condition than in the safe condition. (B) Contrast estimates of the peak voxel in the activated cluster in the right anterior insula for each condition. (C) The time course for BOLD signal change of the peak voxel in the right anterior insula for each condition during the anticipation period. Each line represents the mean event-related BOLD response over all participants for each condition with the standard error of the mean as represented by the area with the corresponding color. The plot was created by using rfxplot

Toolbox (Gläscher 2009).

aIns, anterior insula; PAG, periaqueductal gray; BNST, bed nucleus of the stria terminalis.

Table 2. Brain regions significantly more activated in the attention condition than in the safe condition

Anatomical region	**Cluster size**	**MNI coordinates (mm)**			***T*-value**
		x	**y**	**Z**	
Left red nucleus	516	-6	-25	-9	7.53
Right caudate head		12	5	4	6.31
Left medial dorsal thalamus		-9	-19	13	5.97
Right Inferior frontal gyrus triangular part / anterior insula	105	36	26	7	5.96
Right Inferior frontal gyrus triangular part		48	29	16	3.76

Uncorrected $p < 0.001$ at peak level, family wise error corrected $p < 0.05$ at the cluster level. MNI, Montreal Neurological Institute

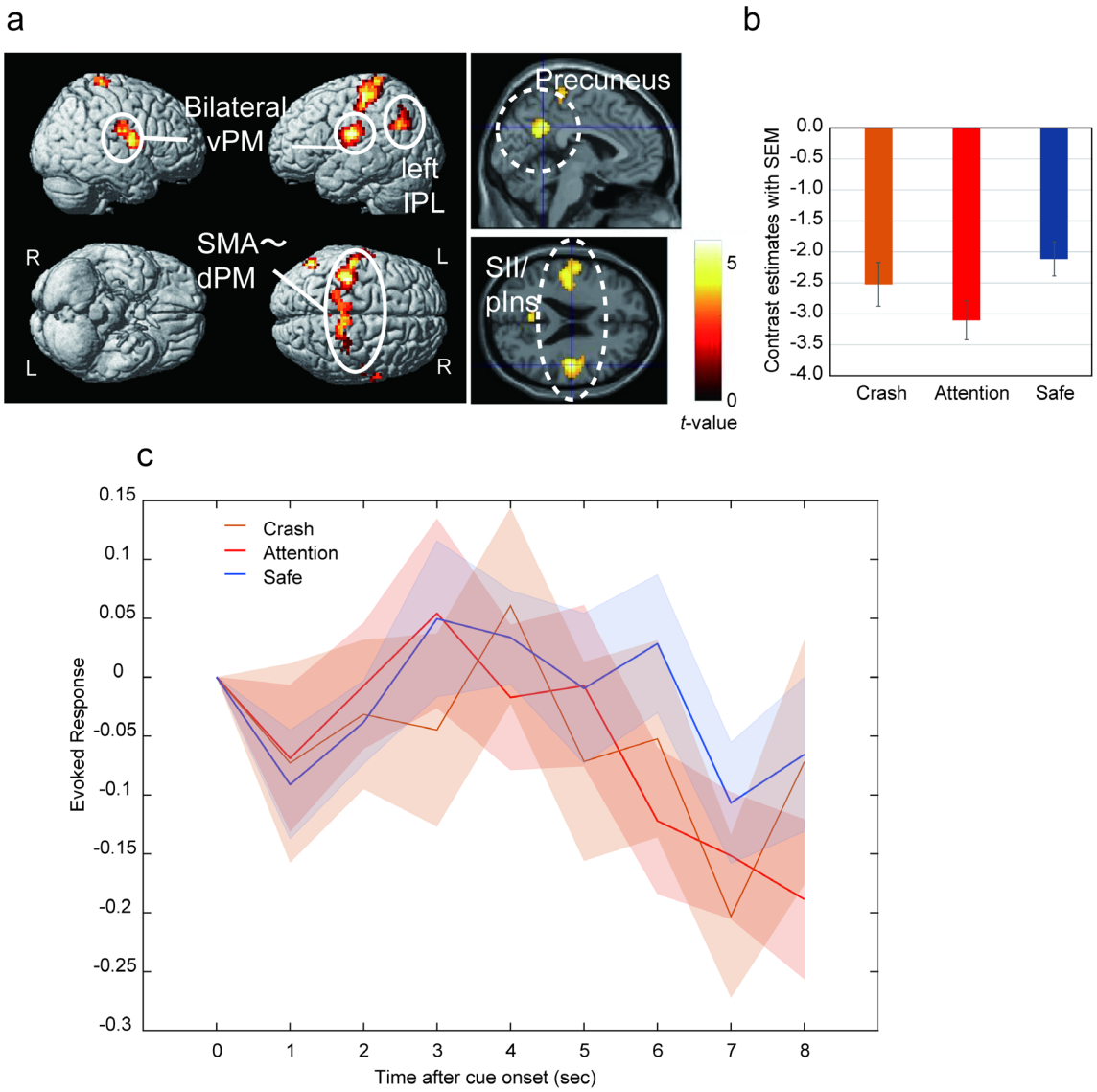

Fig. 9. (A) Brain regions showing more activation in the safe condition than in the attention condition. (B) Contrast estimates of the peak voxel in the activated cluster in the right SII/posterior insula for each condition. (C) The time course for blood oxygenation level-dependent (BOLD) signal change of the peak voxel in the right SII/posterior insula for each condition during the anticipation period. Each line represents the mean event-related BOLD response over all participants for each condition with the standard error of the mean as represented

by the area with the corresponding color. The plot was created by using rfxplot Toolbox (Gläscher 2009).

vPM, ventral premotor cortex; IPL, inferior parietal lobule; SMA, supplementary motor area; dPM, dorsal premotor cortex; SII, secondary somatosensory area; pIns, posterior insula.

Table 3. Brain regions significantly more activated in the safe condition than in the attention condition

Anatomical region	**Cluster size**	**MNI coordinates (mm)**			***T*-value**
		x	**y**	**z**	
Right rolandic operculum	303	48	-13	23	5.70
Right rolandic operculum		60	2	13	5.26
Right posterior insula		39	-10	16	4.99
Left posterior cingulate cortex	110	-3	-52	32	5.10
Left postcentral gyrus	307	-48	-19	26	5.06
Left posterior insula		-39	-13	13	4.95
Left postcentral gyrus		-57	-7	20	4.54
Left inferior parietal cortex	500	-54	-22	48	4.92

Left postcentral gyrus		-42	-34	61	4.74
Right paracentral lobule		6	-31	64	4.74
Left angular gyrus	99	-57	-67	29	4.85
Left angular gyrus		-45	-55	29	4.28
Left angular gyrus	303	-51	-67	42	3.90

Uncorrected $p < 0.001$ at peak level, family wise error corrected $p < 0.05$ at the cluster level. MNI, Montreal Neurological Institute

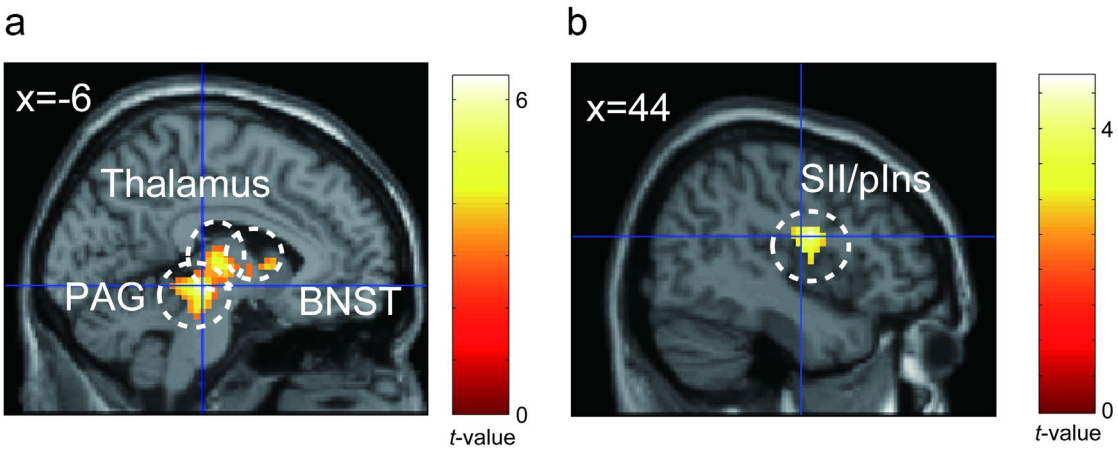

Fig. 10. Brain activation correlated with the anxiety rating scores. (A) Brain regions positively correlated with subjective anxiety (B) Brain regions negatively correlated with subjective anxiety. PAG, periaqueductal gray; BNST, bed nucleus of the stria terminalis; SII, secondary somatosensory area; pIns, posterior insula.

Table 4.

(A) Brain regions showing activation positively correlated with the subjective ratings of anxiety

Anatomical region	Cluster size	MNI coordinates (mm)			*T*-value
		x	y	z	
Left red nucleus	199	-6	-25	-6	6.43
Left medial dorsal thalamus		-3	-19	4	4.49
Left medial dorsal thalamus		-9	-19	10	4.46

Uncorrected $p < 0.001$ at peak level, family wise error corrected $p < 0.05$ at the cluster level. MNI, Montreal Neurological Institute

(B) Brain regions showing activation negatively correlated with subjective ratings of anxiety.

Anatomical region	Cluster size	MNI coordinates (mm)			*T*-value
		x	y	z	
Right rolandic operculum	194	48	-4	20	4.74
Right rolandic operculum		51	-13	23	3.82
Right posterior insula		42	-4	7	3.56

Uncorrected $p < 0.005$ at peak level. MNI, Montreal Neurological Institute

Brain activity related to crash

The contrast in the crash event versus baseline showed extensive brain activation; therefore, we reported the brain regions that survived the threshold of voxel-level FWE corrected $p < 0.05$. The activated regions can be classified into approximately three large clusters (Supplementary Figure S1A, Supplementary Table S1): (1) a posterior midline cluster from the precuneus, cerebellum, and thalamus; (2) a frontal midline cluster including the supplementary motor area and anterior cingulate cortex, and (3) a fronto-temporoparietal cluster including the anterior insula, inferior frontal cortex, superior temporal cortices, parietal operculum, and posterior insula. This fronto-temporoparietal cluster included the amygdala (Supplementary Figure S1B).

Autonomic response-related functional connectivity

Based on the brain activity in the contrast condition (attention > safe), we conducted gPPI analyses using the right anterior insula (dorsal and ventral agranular insula) and the brain regions including the anterior insula cluster, such as right middle frontal gyrus (MFG) ventral

area (Brodmann area [BA] 9/46), right inferior frontal sulcus, right caudal inferior frontal gyrus (IFG) (BA45), right rostral IFG (BA45), and right opercular IFG (BA44) as seed regions.

Regarding the pupil area, although we observed no brain region showing significant FC for the right anterior insula as a seed region, we found brain regions showing significant pupil-related FCs with the adjacent brain areas to the anterior insula: the right MFG and the right rostral IFG (BA45). We found the left cerebellum/brainstem showed a significant pupil-related FC with the right MFG, and the left visual cortex showed a significant pupil-related FC with right rostral IFG (Figure 11A-B, Table 6).

Regarding the β_{art}, we found significant FCs between the right dorsal agranular insula and the middle/posterior cingulate cortex (MCC/PCC) and between the right ventral agranular insula and the right visual cortex (Figure 11C-D, Table 6). In contrast, we found no brain region showing significant FC with the adjacent regions to the anterior insula.

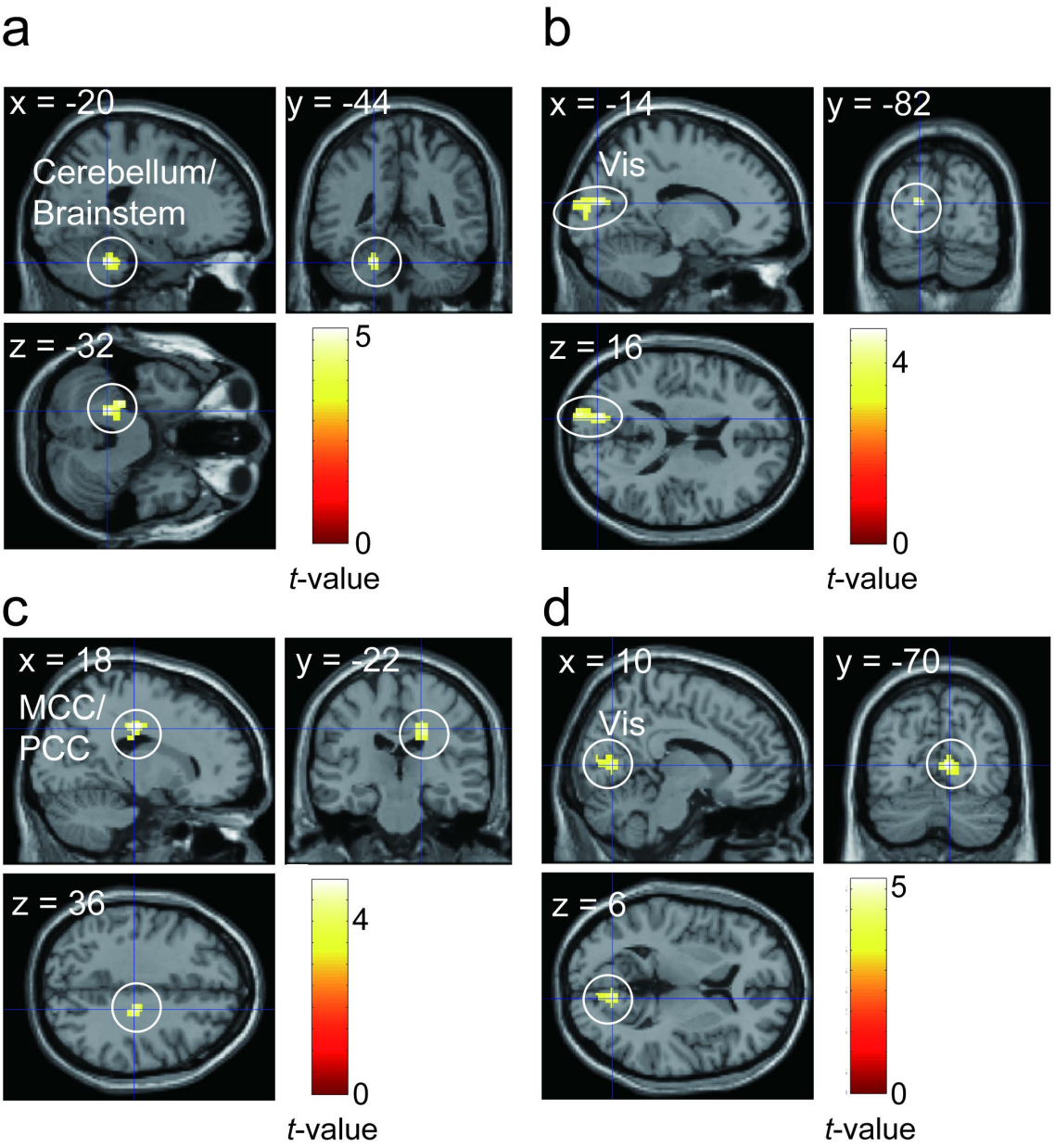

Fig. 11. (A–B) Brain regions showing pupil-related functional connectivity. (A) Brain regions showing pupil-related functional connectivity for the right MFG as seed region. (B) Brain regions showing pupil-related functional connectivity for the right rostral IFG as seed region. (C–D) Brain regions showing peripheral arterial stiffness (β_{art}) -related functional connectivity. (C) Brain regions showing β_{art} -related functional connectivity for the right dorsal agranular insula as seed

region. (D) Brain regions showing β_{art} -related functional connectivity for the right ventral agranular insula as seed region. Vis, visual cortex; MCC, middle cingulate cortex; PCC, posterior cingulate cortex.

Table 6. Brain regions showing pupil-related functional connectivity

(A) Brain regions showing pupil-related functional connectivity for the right MFG as seed region

Anatomical region	**Cluster size**	**MNI coordinates (mm)**			***T*-value**
		x	**y**	**z**	
Left cerebellum	176	-20	-44	-32	5.26
Left cerebellum		-26	-34	-32	5.07
Brainstem		-14	-34	-32	3.50

Uncorrected $p < 0.001$ at peak level, false discovery rate corrected $p < 0.05$ at the cluster level.

MNI, Montreal Neurological Institute

(B) Brain regions showing pupil-related functional connectivity for the right rostral IFG as seed region

Anatomical region	**Cluster size**	**MNI coordinates (mm)**			***T*-value**
		x	**y**	**z**	
Left cuneus	307	-14	-82	16	4.74
Left superior occipital gyrus		-18	-98	16	4.44
Left superior occipital gyrus		-14	-92	12	3.99

Uncorrected $p < 0.001$ at peak level, false discovery rate corrected $p < 0.05$ at the cluster level.

MNI, Montreal Neurological Institute

(C) Brain regions showing β_{art} -related functional connectivity for the right dorsal agranular insula as seed region

Anatomical region	**Cluster size**	**MNI coordinates (mm)**			***T*-value**
		x	**y**	**z**	

White matter	153	18	-22	36	4.94
Middle cingulate gyrus		14	-16	40	4.08
Posterior cingulate gyrus		14	-26	40	3.63

Uncorrected $p < 0.001$ at peak level, false discovery rate corrected $p < 0.05$ at the cluster level.

MNI, Montreal Neurological Institute

(D) Brain regions showing β_{art} -related functional connectivity for the right ventral agranular insula as seed region

Anatomical region	**Cluster size**	**MNI coordinates (mm)**			***T*-value**
		x	**y**	**z**	
Right calcarine sulcus	155	10	-70	6	5.24
Right calcarine sulcus		10	-80	10	4.17
Right lingual gyrus		2	-70	4	3.97

Uncorrected $p < 0.001$ at peak level, false discovery rate corrected $p < 0.05$ at the cluster level.

MNI, Montreal Neurological Institute

Discussion

In this study, we examined the neural basis of anxiety and anxiety-related autonomic responses in a daily driving situation. We hypothesized that the brain network related to the elicitation of anxiety and corresponding autonomic responses would be observed in the anterior insula and sub-cortical regions. As predicted, during the period in which the participants anticipated a car crash, we observed cortico-subcortical activations in the anterior insula, PAG, thalamus, and BNST. We also observed significant pupil dilation and a trend of increase in β_{art} related to the anticipation of a crash. The FC analyses using these autonomic responses revealed that the β_{art} -related FC was found between the right dorsal anterior insula and cingulate cortex, and between the right ventral anterior insula and visual cortex, and that the pupil-related FC was found between the right MFG and the cerebellum/brainstem and between the right rostral IFG and the visual cortex.

Brain regions involved in anxiety elicitation

In the attention condition, the brain regions including the anterior insula, PAG, thalamus, and BNST were more active compared to that of the safe condition. The anterior insula is

reportedly involved in the integration and prediction of interoceptive information (Craig 2009) and in the allostatic process based on prediction (Barrett et al. 2017). The peak voxel of the anterior insula cluster is located at the dorsal part of the anterior insula and extends to the operculum and triangular parts of the inferior frontal gyrus. These areas are consistent with those related to sustained fear reported by Somerville et al. (2013). The dorsal anterior insula has been suggested to be involved in cognitive and attentional functions rather than emotion function (e.g., Chang et al. 2013). This could lead to a claim that the anterior insula activity in the attention condition could reflect only the attentional process. However, this can be ruled out for the following reasons. The results of anxiety ratings indicated that participants felt anxiety more in the attention condition than in the safe condition. In contrast, RTs showed no significant difference between conditions (see Figure 3), suggesting that attentional resources allocated to the task did not differ between the conditions. Furthermore, we found no significant activation in the dorsal attentional network, such as the dorsolateral prefrontal cortex, frontal eye field, and posterior parietal cortex, in the comparison between the attention and safe conditions. Thus, our results suggest that the brain regions, including the anterior insula, were related to anxiety, that is, negative emotion caused by prediction of an aversive event rather than just attention.

PAG receives projections from the prefrontal cortex, insula, and amygdala (Mantyh 1982). The PAG is suggested to play a role in homeostatic defense by integrating afferent

information from the periphery and information from higher centers (Linnman 2012). For instance, PAG is known to be involved in pain modulation. It has been reported that when pre-stimulus functional connectivity between the anterior insula and PAG is stronger, participants perceive a pain stimulus as less painful (Ploner et al. 2010).

The thalamus is also reportedly involved in the modulation of ascending nociceptive information (Tang et al. 2009). Moreover, it is also known that the thalamus relays nociceptive information to the insula, anterior cingulate cortex, and somatosensory cortices (Kummer et al. 2020). In the current study, we observed thalamic activation mainly in the dorsomedial region. Considering that the dorsomedial thalamus is a part of the medial spinothalamocortical pathway involved in nociceptive-specific responses (e.g., Gingold et al. 1991), the thalamic activity observed in this study presumably reflects the anticipatory modulation of responses to unpleasant stimuli accompanied by collision.

The BNST is known to be involved in emotion, threat, and autonomic processing (Davis et al. 2010; Crestani et al. 2013). While animal studies have reported the structural connection between the insula and BNST (e.g., Centanni et al., 2019), the BNST-insula connection in human brains has also been revealed in recent MRI studies (e.g., Avery et al. 2014; Flook et al. 2020). This connection is suggested to be involved in the translation of emotional states into behavioral responses including “fight or flight” (Flook et al. 2020). Based on these previous studies,

activation in the BNST and anterior insula observed in the attention condition might be involved in elicitation of autonomic and behavioral responses accompanied with anticipation of a crash. Thus, our results suggest that a cortico-subcortical network comprising the anterior insula, PAG, BNST, and thalamus is involved in the prediction of negative events and elicitation of anxiety-related responses based on interoceptive information in the attention condition.

In contrast, the SII/posterior insula and precuneus were more activated in the safe condition than in the attention condition. In the attention condition where a crash was predicted, the activation in these regions decreased as the timing of the crash approached (see Figure 9C). Therefore, this deactivation could reflect the allostatic process preparing for the predicted response to a possible upcoming aversive event. The SII/posterior insula has been reported to be involved in processing aversive stimuli (e.g., Apkarian et al. 2005). In particular, the SII has been suggested to represent somatosensory prediction error (Blakemore et al. 1998). In the study by Blakemore et al., participants underwent two experimental conditions in which the experimenter tickled the participants' palms, and the participants tickled themselves. In the condition of self-tickling, the SII was more deactivated than in the condition in which the experimenter tickled them, suggesting that this deactivation reflects the process of canceling out the sensory consequences, that is, a tickly feeling, generated by prediction. Furthermore, crash-related activation overlapped in the SII/posterior insula cluster, as observed in the contrast of safe >

attention. This suggests that SII/posterior insula activation could reflect a part of the aversive sensation elicited by the crash. Considering these observations, the deactivation in the SII/posterior insula observed in the attention condition could be interpreted as an allostatic attenuation triggered by the prediction of sensory input followed by an upcoming aversive event.

The precuneus is part of the default mode network (DMN). It has been proposed that the DMN is switched to the central executive network (CEN) according to the task demand by the SN (Menon and Uddin 2010). Therefore, deactivation in the precuneus could reflect inhibition of the DMN to prepare and pay attention to the upcoming event in the attention condition.

Brain activity related to subjective anxiety

The results of the parametric modulation analyses showed that subjective anxiety significantly correlated with activation in the thalamus and PAG, and not to the anterior insula. This could be explained by the relationship between anterior insula-PAG pre-stimulus functional connectivity and subjective pain sensation (Ploner et al., 2010). Considering that the anterior insula-PAG connection during the anticipation period determines subjective anxiety, when anticipatory modulation of PAG by the anterior insula was insufficient, the participants could have felt more anxious. In contrast, regardless of subjective anxiety, the anterior insula was active when

an upcoming crash could be predicted, which could contribute to the result that the anterior insula was less related to subjective anxiety.

In contrast, the SII/posterior insula showed a tendency for its activity to be negatively related to subjective anxiety, although this was not statistically significant. Considering that the deactivation in the posterior insula reflects an allostatic response based on prediction of sensation to be elicited by an upcoming collision, our results suggest that subjective anxiety decreased when the allostatic process was less involved.

While many previous studies have suggested that the amygdala is involved in anxious emotion, we did not find significant amygdala activity during the anticipation period in the contrast of attention > safe or in the parametric modulation of subjective anxiety. However, the amygdala was significantly active in response to a crash relative to the baseline (Supplementary Figure S1B)[1]. This is consistent with the study of Somerville et al. (2013), who reported that the

[1] We must note that the crash condition was quite different from other conditions as indicated in the behavioral data. For example, the RTs to "STOP" in the crash condition were faster than in other conditions. This could be attributed to the auditory-visual stimuli accompanied with a crash that captured the participants' attention, thereby enhancing their responses to "STOP." Furthermore, the subjective ratings for the crash condition were significantly different from other

amygdala responds to transient fear rather than sustained anxious emotion (anxiety). Thus, in the current study, the absence of amygdala activity during the anticipation phase is reasonable.

Brain regions involved in anxiety-related autonomic responses

The autonomic response-related FC analyses revealed that the right anterior insula and its adjacent regions showed significant FC with visual cortex, cerebellum, brainstem, and MCC/PCC.

Related to β_{art}, the right ventral and dorsal anterior insula showed FC with the visual cortex and MCC/PCC, respectively. The anterior insula controls the autonomic nervous system by regulating the subcortical brain areas, such as the PAG (Thayer and Lane 2009; Critchley and Harrison 2013). Previous research has demonstrated that autonomic control of cardiac activity is lateralized and mediated by the right insular cortex (Colivicchi et al. 2004; Craig, 2009). For instance, evidence from stroke studies has suggested that the right insula plays a major role in

---

conditions, indicating that the subjective ratings performed after each trial were affected by the crash, as predicted.

cardiac autonomic control (e.g., Colivicchi et al. 2004). Craig (2009) proposed a hypothesis that the right and left insula cortices are involved in the control of the sympathetic and parasympathetic nervous systems, respectively. Based on these findings, it is reasonable that the β_{art} -related FC for the right anterior insula as seed region was observed. The MCC/PCC cluster showing the FC with the right dorsal anterior insula was located at the posterior part of the MCC and PCC. Particularly, the PCC is suggested to be involved in controlling the balance between an internal and external attentional focus collaborating with the right anterior insula (Leech and Sharp 2014). The ventral anterior insula, which is involved in affective processing, showed the FC with the visual cortex. This might reflect the allostatic processing of upcoming visual information based on anxiety elicitation. These observations suggest that the allostatic affective processing was associated with the β_{art} change. However, Tsuji et al. (2021) demonstrated that the β_{art} during pain stimulation correlated with the brain activity in the SN, including the dorsal anterior cingulate cortex (dACC), but not the anterior insula. This inconsistency could suggest that the anterior insula is related to the β_{art} attributed to anticipation, whereas the dACC is related to that caused by stimulation.

Regarding the pupil-related FC, the right ventral MFG and the rostral IFG showed FC with the cerebellum/brainstem and the visual cortex, respectively. The brain regions, including the anterior insula/IFG and MFG, have also been reported to be related to pupil change during reward anticipation (Schneider et al. 2018). The ventral MFG and rostral IFG, which are adjacent

to the inferior frontal sulcus, are a part of the ventral attention network (Corbetta et al. 2008). The ventral attention network is known to be a part of the SN and has been suggested to be a "circuit breaker" that reorients focused attention by detecting salient stimuli such as oddballs. The ventral MFG showed an FC with the cluster including the pons located near (however, not including) the locus coeruleus (LC), which is involved in pupil control (Schneider et al. 2016). Furthermore, FC between the IFG and visual cortex was observed. This FC could reflect allostatic attentional control to visual information. Considering that the pupil-related FC for the anterior insula as seed was not observed, the pupil-related FC in the current study could reflect a relatively cognitive aspect of allostatic processing, such as attention control to visual information accompanied by an upcoming collision.

Thus, our results suggest that the anterior insula and its adjacent regions collaborating other regions could differently realize an allostatic attention control and adaptive physiological response to environmental information.

However, we did not observe FC with the brain regions involved in general direct control of the pupil and artery, such as the LC for pupil dilation and the hypothalamus for the artery. One possible interpretation of this result is that the regions observed in this study could be involved in task-evoked modulation of the pupil and artery as part of the allostatic process. During the resting state, for instance, the change rate of pupil diameter is known to be correlated with

BOLD signals in the brainstem (Schneider et al. 2016). However, certain studies have reported that LC activation is not related to task-evoked pupil dilation (Schneider et al. 2018). Nevertheless, the relationship between the task-evoked pupil- and artery-related regions and those involved in the general control of the pupil and artery should be further examined in future research.

Regarding pupil dilation, we found a robust difference between the attention/crash and safe conditions. We also observed a marginal positive correlation between the subjective ratings of anxiety and pupil dilation. These results suggest the possibility that the measurement of pupil dilation is useful in detecting anxiety. However, we must note that the correlation between the arousal ratings and pupil dilation was also marginally significant. Therefore, future studies controlling the arousal level should assess whether pupil dilation merely reflects the arousal or not.

In contrast, β_{art} showed a marginally significant increase in the attention/crash conditions relative to the safe condition. This difference between physiological indices used in the current study could have resulted from their temporal properties. The arousal-related pupil dilation reportedly appears at nearly 200 ms (Sirois et al. 2014). In the current study, owing to the fast latency of pupil dilation, the fluctuation in the participants' subjective emotional state could be reflected more accurately than β_{art}. In contrast to pupil dilation, β_{art} is a relatively newly proposed index. Information on the temporal properties and mechanism of β_{art} should be

investigated in future studies.

Limitations and future directions

In the current study, we demonstrated that the network including the anterior insula plays a pivotal role for eliciting anxiety and for accompanying autonomic responses in a daily situation. However, our results cannot lead to understanding of the clinical situations, such as anxiety disorder. For instance, we found no significant correlation between the trait and state anxiety and the subjective ratings. Furthermore, there was no significant brain activation related to the individual difference in the trait anxiety nor the state anxiety before and after the experiment assessed by STAI. This could be attributed to the fact that we only recruited healthy participants with relatively narrow range of scores. To apply our findings to understanding the anxiety disorder, we should compare brain activity and physiological responses between patients and normal controls. In future studies, we should assess whether anxiety-prone individuals exhibit increase in the pupil area and β_{art}; it will enable us to deepen our understanding on the mechanism of anxiety.

Our results also showed that the increase in pupil area and peripheral arterial stiffness were commonly related to the network including the right anterior insula and its adjacent regions

in a daily situation of driving a vehicle. This suggests that these are potential indices to detect the driver's anxiety during driving underpinned by neuroscientific evidence. However, the experimental environment in the MRI scanner differs much from an actual driving situation. For instance, the participants did not hold a steering wheel or place their foot on a brake pedal. Furthermore, they were lying in a supine position in the MRI scanner. For industrial application, we should conduct an experiment with a realistic steering device (e.g., Okamoto et al. 2020) usable in an MRI scanner. It is also necessary to perform brain imaging and physiological recordings using wearable devices (e.g., Protzak and Gramann 2018) while driving an actual vehicle.

Conclusions

Our results suggest that cortico-subcortical regions, including the right anterior insula, PAG, thalamus, and BNST, play a core role in anticipatory responses to upcoming threats in daily driving situations. We also observed that multiple autonomic responses, such as pupil dilation and β_{art}, were evident when an upcoming threat was predicted, and the right anterior insula and its adjacent regions play a key role in eliciting autonomic responses. These results suggest that pupil dilation and β_{art} reflect anxiety-related SN activity and that they could be potential candidates for

indices for detecting task-evoked anxious emotion based on neuroscientific evidence.

Conflicts of Interest

DS, NM, HY, and MT were employed by Mazda Motor Corporation. TN was also employed by Mazda Motor Corporation during the period when the current study was being conducted. The other authors declare no conflict of interest.

Funding

This work was supported by JST COI (Grant No. JPMJCE1311).

Acknowledgments

We are grateful to Dr. Norihiro Sadato, Dr. Alan Fermin, Dr. Kentaro Ono, Dr. Ayumu Matani, Dr. Toshio Tsuji, and Dr. Maro G. Machizawa for helpful discussions concerning this study, and Ms. Noriko Miura and Ms. Tamami Tomita for assistance with the implementation of the experiment. We would like to thank Editage (www.editage.com) for English language editing.

References

Apkarian AV, Bushnell MC, Treede RD, Zubieta JK. 2005. Human brain mechanisms of pain perception and regulation in health and disease. Eur J Pain. 9:463–484.

Avery SN, Clauss JA, Winder DG, Woodward N, Heckers S, Blackford JU. 2014. BNST neurocircuitry in humans. NeuroImage. 91:311–323.

Barrett LF. 2017. The theory of constructed emotion: an active inference account of interoception and categorization. Soc Cogn Affect Neurosci. 12:1–23.

Barrett LF, Quigley KS, Hamilton P. 2016. An active inference theory of allostasis and interoception in depression. Phil Trans R Soc B. 371:20160011.

Barrett LF, Simmons WK. 2015. Interoceptive predictions in the brain. Nat Rev Neurosci. 16: 419–429.

Bitsios, P, Szabadi E, Bradshaw CM. 2004. The fear-inhibited light reflex: Importance of the anticipation of an aversive event. Int J Psychophysiol. 52:87–95.

Chen WG, Schloesser D, Arensdorf AM, Simmons JM, Cui C, Valentino R, Gnadt JW, Nielsen L, St. Hillaire-Clarke C, Spruance V, Horowitz TS, Vallejo YF, Langevin HM. 2021. The emerging science of interoception: sensing, integrating, interpreting, and regulating signals within the self. Trends Neurosci. 44:3–16.

Blakemore SJ, Wolpert DM, Frith CD. 1998. Central cancellation of self-produced tickle sensation. Nat Neurosci. 1:635–640.

Centanni SW, Morris BD, Luchsinger JR, Bedse G, Fetterly TL, Patel S, Winder DG. 2019. Endocannabinoid control of the insular-bed nucleus of the stria terminalis circuit regulates negative affective behavior associated with alcohol abstinence. Neuropsychopharmacology. 44:526–537.

Chang LJ, Yarkoni T, Khaw MW, Sanfey G. 2013. Decoding the role of the insula in human cognition: Functional parcellation and large-scale reverse inference. Cereb Cortex. 23:739–749.

Choe KW, Blake R, Lee SH. 2016. Pupil size dynamics during fixation impact the accuracy and precision of video-based gaze estimation. Vis Res. 118:48–59.

Chudler EH, Dong WK. 1995. The role of the basal ganglia in nociception and pain. Pain. 60:3–38.

Clark A. 2013. Whatever next? Predictive brains, situated agents, and the future of cognitive science. Behav Brain Sci. 36:181–204.

Colivicchi F, Bassi A, Santini M, Caltagirone C. 2004. Cardiac autonomic derangement and arrhythmias in right-sided stroke with insular involvement. Stroke. 35:2094–2098.

Corbetta M, Patel G, Shulman GL. 2008. The reorienting system of the human brain: from environment to theory of mind. Neuron. 58:306–324.

Craig AD. 2009. How do you feel—now? The anterior insula and human awareness. Nat Rev Neurosci. 10:59–70.

Crestani C, Alves F, Gomes F, Resstel L, Correa F, Herman J. 2013. Mechanisms in the bed nucleus of the stria terminalis involved in control of autonomic and neuroendocrine functions: a review. Curr Neuropharmacol. 11:141–159.

Critchley HD, Harrison NA. 2013. Visceral influences on brain and behavior. Neuron. 77:624–638.

Davis M, Walker DL, Miles L, Grillon C. 2010. Phasic vs sustained fear in rats and humans: Role of the extended amygdala in fear vs anxiety. Neuropsychopharmacology. 35:105–135.

Deane GE. 1964. Human heart rate responses during experimentally induced anxiety. J Exp Psychol. 61:489–493.

DiNuzzo M, Mascali D, Moraschi M, Bussu G, Maugeri L, Mangini F, Fratini M, Giove F. 2019. Brain networks underlying eye's pupil dynamics. Front Neurosci. 13:965.

Epstein S, Roupenian A. 1970. Heart rate and skin conductance during experimentally induced anxiety: The effect of uncertainty about receiving a noxious stimulus. J Pers Soc Psychol.

16:20–28.

Fan L, Li H, Zhuo J, Zhang Y, Wang J, Chen L, Yang Z, Chu C, Xie S, Laird AR, Fox PT, Eickhoff SB, Yu C, Jiang T. 2016. The Human Brainnetome Atlas: A New Brain Atlas Based on Connectional Architecture. Cereb Cortex. 26: 3508–3526.

Flook EA, Feola B, Avery SN, Winder DG, Woodward ND, Heckers S, Blackford JU. 2020. BNST-insula structural connectivity in humans. NeuroImage. 210:116555.

Friston K. 2005. A theory of cortical responses. Phil Trans R Soc B. 360:815–836.

Gingold SI, Greenspan JD, Apkarian AV. 1991. Anatomic evidence of nociceptive inputs to primary somatosensory cortex: relationship between spinothalamic terminals and thalamocortical cells in squirrel monkeys. J Comp Neurol. 308:467–490.

Gläscher J. 2009. Visualization of group inference data in functional neuroimaging. Neuroinformatics. 7:73–82.

Grupe DW. Nitschke JB. 2013. Uncertainty and anticipation in anxiety: An integrated neurobiological and psychological perspective. Nat Rev Neurosci. 14:488–501.

Kummer KK, Mitrić M, Kalpachidou T, Kress M. 2020. The medial prefrontal cortex as a central hub for mental comorbidities associated with chronic pain. Int J Mol Sci. 21:3440.

Leech R, Sharp DJ. 2014. The role of the posterior cingulate cortex in cognition and disease. Brain. 137:12–32.

Linnman C, Moulton EA, Barmettler G, Becerra L, Borsook D. 2012. Neuroimaging of the periaqueductal gray: State of the field. NeuroImage. 60:505–522.

Mantyh PW. 1982. Forebrain projections to the periaqueductral gray in the monkey, with observations in the cat and rat. J Comp Neurol. 211:146–158.

Matsubara H, Hirano H, Hirano H, Soh Z, Nakamura R, Saeki N, Kawamoto M, Yoshizumi M, Yoshino A, Sasaoka T, Yamawaki S, Tsuji T. 2018. Quantitative evaluation of pain during electrocutaneous stimulation using a log-linearized peripheral arterial viscoelastic model. Sci Rep. 8:3091.

Menon V, Uddin LQ. 2010. Saliency, switching, attention and control: a network model of insula function. Brain Struct Funct. 214:655–667.

Michel F, Henaff M. 2004. Seeing without the occipito-parietal cortex: Simultagnosia as a shrinkage of the attentional visual field. Behav Neurol. 15:3–13.

Okamoto Y, Sasaoka T, Sadato N, Fukunaga M, Yamamoto T, Soh Z, Nouzawa T, Yamawaki, S, Tsuji T. 2020. Is Human Brain Activity during Driving Operations Modulated by the Viscoelastic Characteristics of a Steering Wheel?: An fMRI Study. IEEE Access. 8:

215073–215090.

Paulus MP, Stein MB. 2006. An insular view of anxiety. Biol Psychiatry. 60:383–387.

Paulus MP, Stein MB. 2010. Interoception in anxiety and depression. Brain Struct Funct. 214:451–463.

Ploner M, Lee MC, Wiech K, Bingel U, Tracey I. 2010. Prestimulus functional connectivity determines pain perception in humans. Proc Natl Acad Sci U S A. 107:355–360.

Protzak J, Gramann K. 2018. Investigating established EEG parameter during real-world driving. Front. Psychol. 9:2289.

Rao RPN, Ballard DH. 1999. Predictive coding in the visual cortex- a functional interpretation of some extra-classical receptive-field effects. Nat Neurosci. 2:79–87.

Schneider M, Leuchs L, Czisch M, Sämann PG, Spoormaker VI. 2018. Disentangling reward anticipation with simultaneous pupillometry / fMRI. NeuroImage. 178:11–22.

Seth AK. 2013. Interoceptive inference, emotion, and the embodied self. Trends Cogn Sci. 17:565–573.

Sirois S, Brisson J. 2014. Pupillometry. Wiley Interdisciplinary Reviews: Cognitive Science. 5:679–92.

Somerville LH, Wagner DD, Wig GS, Moran JM, Whalen PJ, Kelley WM. 2013. Interactions between transient and sustained neural signals support the generation and regulation of anxious emotion. Cereb Cortex. 23:49–60.

Strange BA, Dolan RJ. 2007. β-adrenergic modulation of oddball responses in humans. Behav Brain Funct. 3:29.

Tang JS, Qu CL, Huo FQ. 2009. The thalamic nucleus submedius and ventrolateral orbital cortex are involved in nociceptive modulation: A novel pain modulation pathway. Prog Neurobiol. 89:383–389.

Thayer JF, Lane RD. 2009. Neuroscience and Biobehavioral Reviews Claude Bernard and the heart–brain connection: Further elaboration of a model of neurovisceral integration. Neurosci Biobehav Rev. 33:81–88.

Tsuji T, Arikuni F, Sasaoka T, Suyama S, Akiyoshi T, Soh Z, Hirano H, Nakamura R, Saeki N, Kawamoto M, Yoshizumi M, Yoshino A, Yamawaki S. 2021. Peripheral arterial stiffness during electrocutaneous stimulation is positively correlated with pain related brain activity and subjective pain intensity: an fMRI study. Sci Rep. 11:4425.

Wager TD, Waugh CE, Lindquist M, Noll DC, Fredrickson BL, Taylor SF. 2009a. Brain mediators of cardiovascular responses to social threat. Part I: Reciprocal dorsal and ventral sub-

regions of the medial prefrontal cortex and heart-rate reactivity. NeuroImage. 47:821–835.

Wager TD, van Ast VA, Hughes BL, Davidson ML, Lindquist MA, Ochsner KN. 2009b. Brain mediators of cardiovascular responses to social threat, Part II: Prefrontal-subcortical pathways and relationship with anxiety. NeuroImage. 47:836–851.

Whitfield-Gabrieli S, Nieto-Castanon A. 2012. Conn: A functional connectivity toolbox for correlated and anticorrelated brain networks. Brain Connect. 2: 125–141.

Yeo SS, Chang PH, Jang SH. 2013. The ascending reticular activating system from pontine reticular formation to the thalamus in the human brain. Front Hum Neurosci. 7:416.